

Theoretical Evaluation of Axial Induction Factor and Pressure Distribution on Wind Turbine Blades

Vasishtha Bhargava¹, Ch Koteswara Rao², Balaji Krushna .P³

^{1,2,3}Assistant Professors, Department of Mechanical engineering, GITAM University, Hyderabad T.S. India

Email : vasishtab@gmail.com

Abstract: *In this paper BEM& Glauert theory of momentum are investigated for the magnitude of axial induction factor, thrust coefficients and axisymmetric pressure distribution by Kinner. The axial induction factor characteristic is analyzed around the rotor blade in order to determine the extent of velocity gradient in the flow stream relative to free stream. The influence of yaw and wake skew angles on the power coefficient of turbine is analyzed in order to understand the axial induction factor, flow direction from tip of blades in the wake stream and when blade passes the tower. The lift and drag coefficients vary with tip speed ratios and angle of attack and enables to determine the behavior of axial and tangential induction factor observed at different blade locations. The axial induction factor is verified also according to the azimuthal averaged positions of the turbine rotor during the operation.*

Keywords: *Blade Element Momentum, Thrust coefficient, Pressure distribution, Yaw angle, Axial Induction factor, Angle of attack.*

Nomenclature: TSR – Tip speed ratio, AOA – Angle of Attack, BEM – Blade Element Momentum

1. Introduction

Wind turbine operation involves several processes and undergoes static and dynamic loads during its life. The structural components like the gearbox, tower, blades, and hub are subjected to wear and tear as a result. This paper focuses on rotor thrust force and pressure gradient distributions investigated according to different aerodynamic theories (see Kinner, Glauert momentum and axial momentum) [i]. In particular the variables like rotor thrust, axial induction factor and pressure distribution along blade sections which are considered essential to understand the aerodynamic properties and loads on the turbine blades.

2. Literature review

In the past several theories have been developed to predict the thrust force acting on the blades which influence the torque developed by the rotor. BEM based methods are dependent upon the momentum of the air flow across the rotor disc and treat the air particle kinetic energy imparted to the rotor. The change in the momentum as a result will influence the power extraction

capability or the efficiency of a turbine. The magnitude of the change in the velocity is often measured using the induction factor, a , which changes along the length of blade and also the air flow downstream of the rotor during the operation. Other theories such as the vortex based method consider the vortices being developed from the tip and root hub that shed in the form of cylinders and helical vortices during operation. Analytical expressions involved to predict the thrust as well as efficiency C_p that depends on the axial induction factor, yaw angle, and inflow angles. Figure 1 shows the comparison of thrust prediction from BEM based method and Glauert momentum theory [ii]. Under uniform blade circulation, the breakdown of momentum theory is observed at axial induction factor of 0.5 where the thrust decreases according to BEM while for Glauert momentum theory the thrust coefficient keeps rising. Several factors attributed to the increased thrust from Glauert prediction were related with the flow field around the turbine rotor involving the axial, tangential and radial flow field directions.

3. Methodology

The pressure distribution around an airfoil is evaluated using the Legendre polynomial functions presented by Kinner (1938). The aerodynamic loading of the rotor is solved using the elliptical coordinates to determine the pressure. The forces acting on the structural components depend upon blade azimuth angle position, distance of wake downstream and yaw angle of rotor. The change in axial induced velocity is factored at different tip speed ratios to measure the inflow angle along the blade span. The flow over the airfoil can be classified commonly into three stages

- Fully attached flow for which the angle of attack (AOA) is in range of 0-8 deg
- Stalled flow for which angle of attack is in range of 8-12 deg
- Fully separated flow for which angle of attack is in range of 12-16 deg

The angle of attack on an airfoil determines the magnitude of lift and drag coefficients produced on the blade span. The lift and drag forces act orthogonally to the blade span surface. The relative magnitude of these forces changes according to the angle of attack from inboard airfoils ($2/3^{\text{rd}}$) to outboard airfoils. Further, it can be noted that the angle of attack decreases towards the tip for higher blade tip speed ratios, along the blade

span. This trend can be observed for most of the NACA cambered airfoils [vi] used in aircraft wings however, they are also applicable to wind turbine blades. The resultant force tends to produce torque from the turbine.

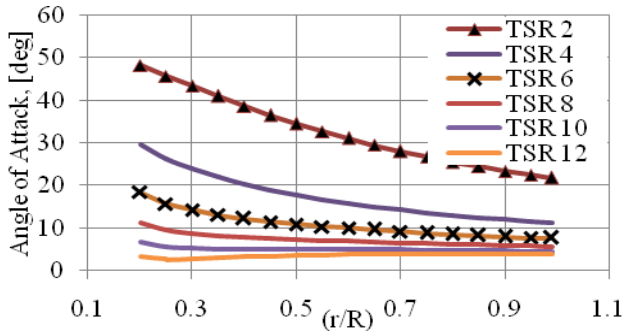


Figure 1 Variation of angle of attack at different TSR along the normalized blade span

The angle of attack (AOA) is given by the equation as shown below, where β is the twist angle, ϕ is the inflow angle at the blade section.

$$\alpha = \phi - \beta \quad (1)$$

$$\phi = \tan^{-1} \left[\frac{1}{\left(\frac{r}{R}\right)\lambda} \right] \quad (2)$$

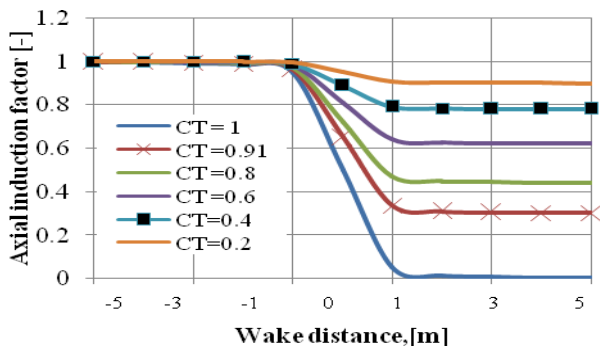


Figure 2 Variation of axial induction factor with wake distance at different thrust levels on rotor

Figure 2 shows the axial induction factor at different wake distance locations in front and behind the rotor. It can be noted that the flow stream in front of turbine is undisturbed and therefore, the axial induction factor is constant with no change in velocity. However, as the thrust coefficients increase on the rotor and at varying wake distances behind the rotor, the axial induction factor is significantly changed within the +/- 1D rotor wake distance. Beyond the 1D wake distance the axial induction factor remains steady. This characteristic is seen due to the ignoring of wake expansion behind the rotor as assumed by the BEM theory. The effect of wake rotation is observed only within the 1D wake distance which results in high reduction of axial induction factor. The thrust coefficients on rotor also vary at different tip speed ratios local to blade which is function of angle

of attack. The analytical relationship expressing the wake distance and axial induction factor is [v]

$$\alpha = \left[1 - \left[\frac{1-a'}{2} \right] \cdot \left\{ 1 + \frac{2\epsilon}{\sqrt{1+4\epsilon^2}} \right\} \right] \quad (3)$$

$$a' = \sqrt{1 - C_T} \quad (4)$$

Where a' is the tangential induction factor, ϵ is the wake distance upstream and downstream of rotor, C_T is the thrust coefficient on the rotor disc using the BEM theory. From BEM theory prediction, the efficiency reaches maximum for axial induction factor of $a=1/3$ and at $a=0.5$ the momentum theory break down occurs at which the thrust coefficients on rotor disc reach maximum value that leads to heavy blade loading. However, the Glauerts momentum theory considers the increased thrust on rotor which continues up to 2.0 and under predicts the efficiency [iii]. The general momentum and BEM theory considers the following assumptions for the flow field

1. Incompressible flow or inviscid flow
2. Finite number of blades Vs infinite rotor solidity
3. Wake skew angle behind the rotor is more than twice the yaw angle
4. No wake rotation behind the rotor disc and divided into discrete annular ring sections vs continuous disc. Forces and resulting moments acting on each blade station are summed up iteratively to calculate the aerodynamic blade loading of the rotor.

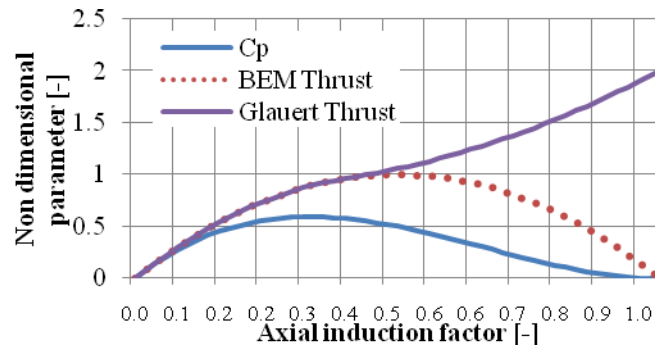


Figure 3 Comparison of BEM thrust and Glauert thrust coefficients

Table1. Turbine blade geometry specifications

Number of blades	3
Rotor radius	17m
Blade root radius	20 % of tip radius
Chord length	1.085m - 0.845m for $0.2 \leq r/R \leq 0.5$ 0.845 - 0.485m for $0.5 \leq r/R \leq 0.95$
Blade twist angle	15 - 3.9 deg for $0.2 \leq r/R \leq 0.5$ 3.9 - 0.2 deg for $0.5 \leq r/R \leq 0.95$
Aerofoil profiles	NACA 0012, NACA 4412, NACA632xx series

4. Results and Discussion

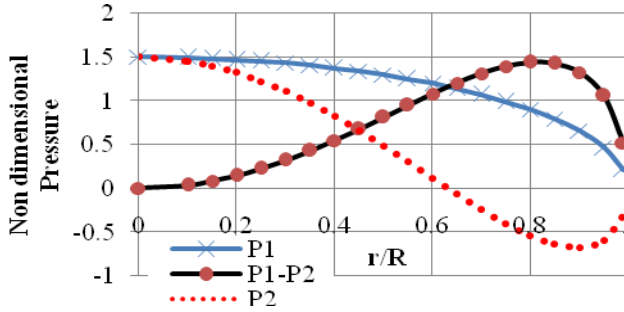


Figure 4 Pressure distributions, along the blade span, as predicted by Kinner

The pressure distribution along the blade span as predicted by Kinner shows the pressure field around the actuator disc. It is based upon the method of accelerating potential flow and derived from Euler equations. The induced velocities are small compared to free stream flow velocity. The pressure gradient across the disc edge is zero according to Kinner (1937) and based upon the Euler's equation in which the velocity is obtained by integrating the acceleration of flow field around the actuator disc. The pressure distribution for the turbine rotor is obtained using the following procedure

- Transformation of Cartesian coordinates into ellipsoidal coordinate system, *ellipsoidal parameter and coordinate and azimuth angle of blade.*
- The pressure field expressed as product of three polynomial functions
- The pressure functions are solved as Legendre polynomial differential equations (van Bussel 1995) for odd and even values to obtain
 - Pressure gradient across the disc i.e. along the blade span, P1
 - The axisymmetric pressure distribution for upstream and downstream of rotor, P2

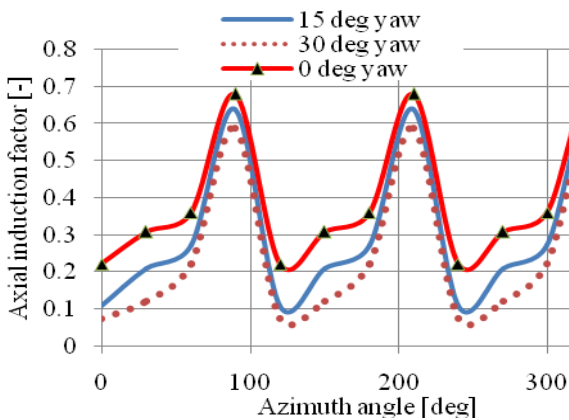


Figure 5 Axial induction factors at TSR of 6 for 0, 15 & 30 deg yaw angles at 0.9R. The blades pass at 90, 210 and 330 degrees.

The combined pressure distribution for which the maximum efficiency is obtained using uniform pressure field conditions. P1-P2

$$\text{The pressure is expressed as [i] } p_1 = \frac{3}{2} C_T \sqrt{1 - \left(\frac{r}{R}\right)^2} \quad (5)$$

$$p_2 = -\frac{3}{4} C_T \sqrt{1 - \left(\frac{r}{R}\right)^2} \left(5 \left(\frac{r}{R}\right)^2 - 2\right) \quad (6)$$

$$p_{1-2} = \frac{15}{4} C_T \left(\frac{r}{R}\right)^2 \sqrt{1 - \left(\frac{r}{R}\right)^2} \quad (7)$$

It must be noted that pressure discontinuity across the rotor disc is discontinuous and the pressure drop is observed to zero at the edge of disc and the hub center ignoring the tip loss effects. The coefficients used in the polynomial functions for pressure variable is dependent upon the thrust coefficient. The axial induced velocity can be used to determine the blade section angle of attack and normal to rotor disc for yawed rotor conditions. The azimuth averaged axial induction factor is calculated at every blade station and at various tip speed ratios. The blade positions are estimated at 90 deg, 210 deg & 330 deg with a phase difference of 120 deg. Hence the solution for a is obtained by the iteration at different yaw angles at the normalized blade radius until the value of a reaches peak of ~ 0.69 and a trough of ~ 0.12, for yawed and unyawed conditions. However, it can be noted the extent of reduction in axial velocity is observed higher for large yaw angles.

The BEM based methods predict the axial induction factor with changing azimuth angle of rotor blades. The blade 1 pass the tower at 90 deg, blade 2 position at 210 deg, blade 3 position at 330 deg respectively. The axial induction factor is dependent upon the wake skew angle, rotor azimuth position, blade solidity and also varies radially which is expressed as following equation below [iv] a_0 is the initial value for axial induction factor equal to 0.

$$a = a_0 [1 + K \cdot F(\theta) \sin \delta] \quad (8)$$

$$K = 2 \tan \frac{\theta}{2} \quad (\text{Coleman formulation}) \quad (9)$$

$$F(\theta) = \theta + 0.4\theta^3 + 0.6\theta^5 \quad (10)$$

$$\theta = \frac{r}{R} \quad (11)$$

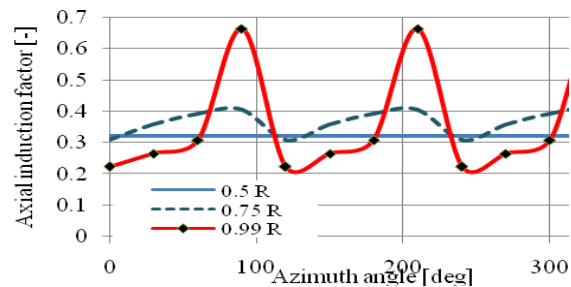


Figure 6 Axial induction factor at TSR of 6 for 0, deg yaw angles at 0.5R, 0.75 R & 0.99R.

The blades pass at 90, 210 and 330 degrees.

The performance coefficient, C_p is evaluated using the BEM theory for various yaw angle positions of the rotor and expressed in terms of yaw angle and axial induction factor using the equation shown below [i] where γ is the yaw angle, a is the axial induction factor.

$$C_p = 4a[\cos\gamma - a]^2 \tag{12}$$

The inflow angle seen by the blade section varies with local tip speed ratio for optimum operation at which axial induction factor is 1/3 is expressed as [i]

$$\phi = \tan^{-1} \left[\frac{1 - \frac{1}{3}}{\left(\frac{r}{R}\right)\lambda \left(1 + \frac{2}{3\left(\frac{r}{R}\right)^2}\right)} \right] \tag{13}$$

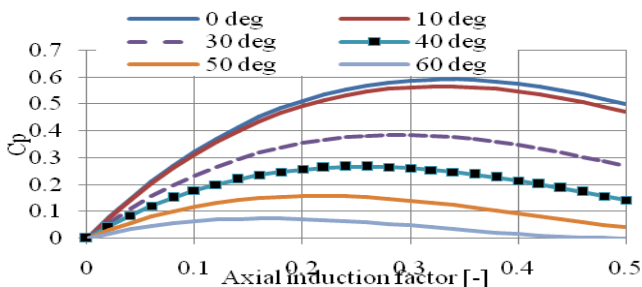


Figure 7 Turbine efficiency variation with yaw angles using BEM based method

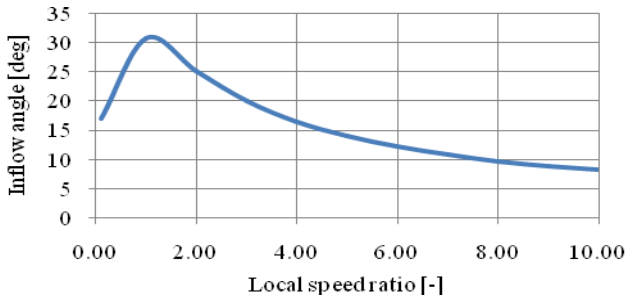


Figure 2 Variation of inflow angle with local tip speed ratio without tip loss in optimum operation

It can be noted that for variable speed turbines, the rotational speed range changes over the wide range at which turbine produces power. Under zero yaw conditions, and without tip loss, the speed ratio and inflow angle vary according to shown in figure 8. Therefore, as the speed ratio increases, the inflow angle at the blade section increases and reaches maximum value at relatively high wind speeds. However the angle of attack is affected due to the blade twist along the blade span as it tends to produce lower lift and thrust force for lower angles. In yawed conditions of turbine, the inflow angle is seen decreasing as the wind speed decreases. This results in reduced C_p of machine as seen from figure 7. In case of fixed speed turbines, the rotational speed is nearly constant and the local speed ratio is function of

only the relative wind speed and blade radius whereas in variable speed machines, the rotational speed governs the maximum operating efficiency of the turbine.

5. Conclusion

The axial induction factor represents the change in the axial velocity along the rotor axis, and expresses the aerodynamic flow on the blade during yawed and unyawed conditions of turbine. Studies were performed to understand the influence of rotor thrust on axial induction factor and its variation on blade span. The yawed rotor conditions influence the magnitude of axial, tangential induction factors and turbine efficiency. Increasing yaw angles reduce the magnitude of turbine efficiency. The axisymmetric pressure distributions are used to analyze the blade loading of rotor upstream and downstream directions with uniform flow conditions. The flow properties like angle of attack, inflow angles enable to estimate the induction factors which drop to zero at the tip of blade at higher local speed ratios

6. References

- i. *Wind energy handbook.* Tony Burton, Nick Jenkins, David Sharpe, Ervin Bossanyi. John Wiley & Sons
- ii. <https://www.irphe.fr/IMG/pdf/Wind-turbine-aerodynamics.pdf>
- iii. www.tudelft.nl/fileadmin/UD/MenC/Support/.../PhD_Thesis_Tonio_Sant.pdf
- iv. www.lr.tudelft.nl/fileadmin/Faculteit/LR/...en.../Vipul_Gupta_r1.pdf
- v. *Aerodynamics of wind turbine wakes* B. Sanderse , ECN –E-09-016,
- vi. www.montana.edu/.../Manwell%20Wind%20Energy%20Explained%20Solutions.pdf